Universitat Autònoma de Barcelona

# Robustness aspects of Model Predictive Control

## Appendices B and C

A DISSERTATION SUBMITTED IN
PARTIAL FULFILMENT FOR THE DEGREE OF
DOCTOR OF PHILOSOPHY AT THE
UNIVERSITAT AUTÒNOMA DE BARCELONA

David Megías Jiménez

March 2000

# Appendix B

# Control of an isothermal chemical reactor

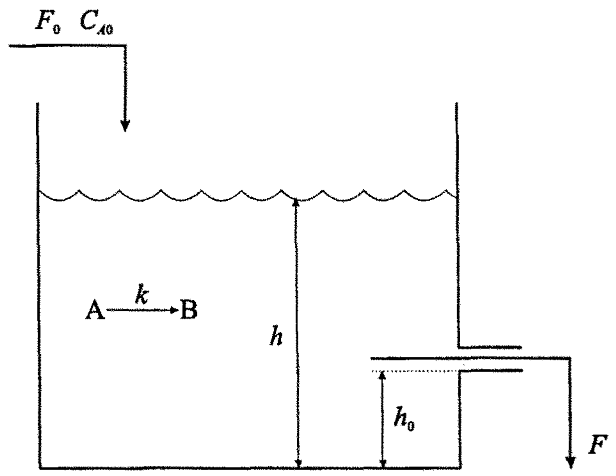


Figure B.1: Isothermal chemical reactor with variable height

In this appendix, the min-max GPC$^\infty$ suggested in Chapter 4 is tested on the isothermal chemical reactor displayed in Fig.B.1. An overview of chemical reactors can be found in (Luyben, 1990).

In this reactor, a chemical A reacts producing some chemical B and the temperature inside the tank is assumed constant, hence the name isothermal. A (volumetric) flow $F_0$ enters the tank with an initial concentration $C_{A0}$ of the product A, and an output flow $F$ is obtained, composed by a mixture of the chemicals A and B. The concentrations of

A and B, $C_A$ and $C_B$ respectively, are assumed uniform within the reactor. The height and the volume of liquid in the tank are variable and reach the steady-state value when the input and the output flows become identical, *i.e.* $F = F_0$. The control objective is to achieve a specified setpoint of the concentration $C_B$ by manipulating the input flow $F_0$, satisfying the input and output constraints $F_0 \geq 0$ and $C_B \leq C_B^+$.

The transformation of A into B is determined by the reaction rate $k$, which can be computed from the Arrhenius equation:

$$k = k_0 \mathrm{e}^{-E_A/RT_l},$$

where $k_0$ is a constant, $E_A$ is the activation energy, $T_l$ is the absolute temperature in the tank and $R$ is the perfect-gas constant. The output flow of the tank $F$ is proportional to the square root of the pressure drop in both sides of the pipeline, which reduces to the formula

$$F = \begin{cases} 0 & \text{if } h < h_0, \\ K_F\sqrt{h - h_0} & \text{if } h \geq h_0, \end{cases}$$

for some constant $K_F$.

The height $h$ dynamics can be easily obtained from the input and output flows. Let $V = Ah$ denote the volume of liquid in the tank, where $A$ is the area of the base and $h$ is the fluid height, then it follows that

$$\frac{dV}{dt} = A\frac{dh}{dt} = F_0 - F$$

Finally, the mass balance equations can be obtained, from the mass conservation principle, as

$$\begin{aligned} \frac{dM_A}{dt} &= F_0 C_{A0} - FC_A - AhkC_A, \\ \frac{dM_B}{dt} &= -FC_B + AhkC_A, \end{aligned} \tag{B.1}$$

where $M_A$ and $M_B$ denote the masses of A and B respectively and $AhkC_A$ is the quantity of $A$ which reacts giving the substance B. Now, using the relation $M_A = VC_A$, the derivative of $M_A$ can be written as

$$\frac{dM_A}{dt} = \frac{dVC_A}{dt} = C_A\frac{dV}{dt} + V\frac{dC_A}{dt} = C_A A\frac{dh}{dt} + V\frac{dC_A}{dt} = C_A(F_0 - F) + V\frac{dC_A}{dt},$$

and, combining this expression with eqn.B.1, it follows that

$$\begin{aligned} Ah\frac{dC_A}{dt} &= F_0C_{A0} - FC_A - AhkC_A - (F_0 - F)C_A, \\ &= F_0C_{A0} - F_0C_A - AhkC_A. \end{aligned}$$

Likewise, the mass balance of B yields the equation

$$Ah\frac{dC_B}{dt} = -F_0C_B + AhkC_A.$$

In summary, the dynamics of the system depicted in Fig.B.1 are provided by the following differential and algebraic equations:

$$\begin{aligned} Ah\frac{dC_A}{dt} &= F_0C_{A0} - F_0C_A - AhkC_A, \\ k &= k_0 e^{-E_A/RT_l}, \\ Ah\frac{dC_B}{dt} &= -F_0C_B + AhkC_A, \\ A\frac{dh}{dt} &= F_0 - F, \\ F &= \begin{cases} 0 & \text{if } h < h_0, \\ K_F\sqrt{h - h_0} & \text{if } h \geq h_0. \end{cases} \end{aligned}$$

The following parameters have been used for this example: $K_F = 19.9360$, $k_0 = 6700$ $\text{h}^{-1}$, $E_A = 25000$ kJ/kmole, $T_l = 300$ K, $R = 8.414$ kJ/kmoleK, $C_{A0} = 8$ kmole/m$^3$ and $h_0 = 10$ m. The non-linear dynamics of such a reactor are determined by the products of the different state variables in the differential equations. In addition, note that the output flow is given by the non-linear law $F = K_F(h - h_0)^{\frac{1}{2}}$.

Now, a linearised model about the steady-state point $\overline{C_A} = 4$ kmole/m$^3$, $\overline{C_B} = 4$ kmole/m$^3$, $\overline{h} = 15$ m and $\overline{F_0} = 44.5782$ m$^3$/h is obtained. Such a model, discretised with a sampling time of $T_s = 1$ h and adding a ZOH at the input, becomes the transfer function

$$G(q^{-1}) = \frac{q^{-1}B(q^{-1})}{A(q^{-1})} = \frac{-0.0173q^{-1} + 0.0149q^{-2}}{1 - 1.1922q^{-1} + 0.3534q^{-2}},$$

which is used by the MPC controllers of this example.

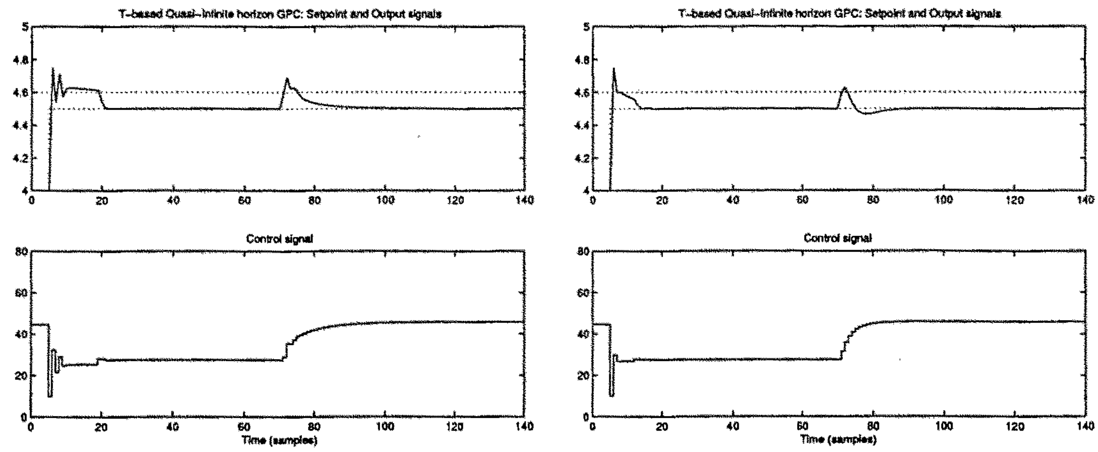


(a) $T = T_2$ (b) $T = T_3$

Figure B.2: Input/Output responses for the $T$-based QGPC$_1^\infty$ (solid), and output constraint (dotted) for $T = T_2$ and $T = T_3$

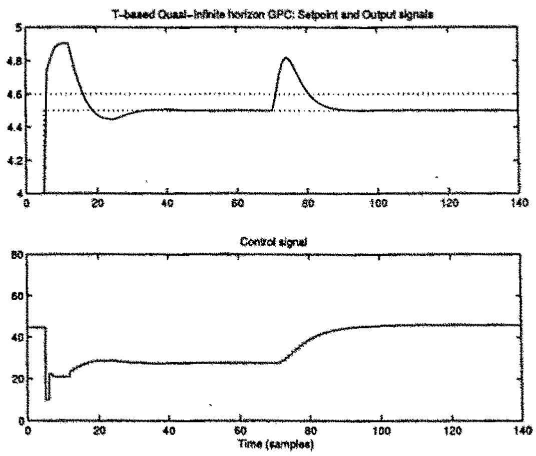


Figure B.3: Input/Output responses for the $T$-based QGPC$_1^\infty$ (solid), and output constraint (dotted) for $T = T_4$

In the next few experiments, the setpoint of $C_B$ is changed from 4 to 4.5 kmole/m$^3$ at time $t = 5$ h (samples), subject to the constraints $F_0 \geq 0$ and $C_B \leq 4.6$ kmole/m$^3$

for all $t$. Note that the output constraint is placed quite near the setpoint, what makes it difficult to fulfil the specifications. In addition a disturbance affects the temperature $T_l$ (and consequently the reaction dynamics $k$) at time $t = 70$ h (samples). This disturbance is determined by $T_l = 300 + 8(1 - e^{70-t})$, *i.e.* at time $t = 71$ h the temperature is a bit greater than 305 K whereas at time $t = 75$ h it reaches the steady-state value $T_l = 308$ K.

Both the $T$-based and the min-max QGPC$_1^\infty$ have been tested with the tuning settings $[N_u, \rho] = [5, 1]$. For the $T$-based controller, four classical choices of the $T$ polynomial, namely $T_1 = 1$, $T_2 = 1 - 0.9q^{-1}$, $T_3 = A$ and $T_4 = A(1 - 0.9q^{-1})$, have been used, whereas the min-max controller has been implemented with the tuning settings $M_\theta = 10$, $\mu = 0.9$, $\theta^-(5) = -0.15$ and $\theta^+(5) = 0.15$.

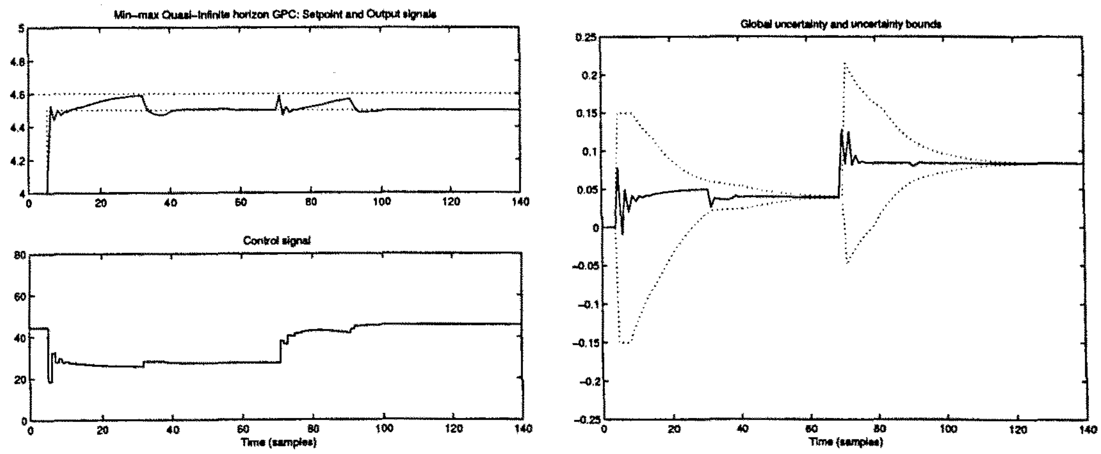


(a) Input/Output responses for the min-max QGPC$_1^\infty$ (solid) and output constraint (dotted)

(b) Global uncertainty (solid) and uncertainty bounds (dotted)

Figure B.4: Closed-loop behaviour for the min-max QGPC$_1^\infty$

The results obtained with the $T$-based controllers are shown in Fig.B.2 and B.3. The optimisation problem with $T = T_1$ becomes unfeasible shortly after the setpoint change, leading to a permanent oscillation (instability) with many constraint violations and thus it is not included in the figure. It is worth pointing out that all these choices of the polynomial $T$ produce constraint violations *although the internal predictions always meet the input/output constraints.* These violations occur both after the setpoint change and the disturbance in $T_l$.

Fig.B.4(a) shows that the min-max controller reaches the setpoint and satisfies the constraint specifications even after the disturbance in $T_l$. It can be observed in Fig.B.4(b) that when the disturbance affects the process the measurements of $\theta(t)$ make it possible to modify the uncertainty bands. Despite the oscillations, the uncertainty signal is kept between the bounds, leading to constraint satisfaction. The final convergence of the lower and upper bands to the steady-state value of $\theta(t)$ leads to offset-free setpoint tracking.

# Appendix C

# Control of a non-isothermal continuous stirred-tank reactor

The min-max and the $T$-based QGPC$_1^\infty$ have been tried on a non-isothermal CSTR. This process is similar to the one presented by Zheng (1999), but the dynamics of the temperature of the coolant in the jacket have been considered. Similarly as for the reactor presented in Appendix B, a chemical product A reacts producing B, but now this reaction is exothermic and gives rise to heat energy which makes the temperature $T_l$ within the tank increase. In order to keep the temperature within the reactor constant (and safe), the tank is covered by a jacket in which a coolant absorbs the heat produced by the reaction. This kind of reactor is designed in such a way that the volume of liquid in the tank $V_l$ and in the jacket $V_r$ are kept constant. The control aim is to change the tank's temperature $T_l$ manipulating the coolant flow $F_r$ satisfying input ($F_r \geq 0$) and output ($T_l \leq T_l^+$) constraint specifications.

The equations describing this process are given below:

$$
\begin{aligned}
V\frac{dC_A}{dt} &= FC_{A0} - FC_A - VkC_A,\\
k &= k_0 \mathrm{e}^{-E_A/RT_l},\\
V\rho C\frac{dT_l}{dt} &= F\rho C(T_{l0} - T_l) - UA(T_l - Tr) + \Delta HVkC_A,\\
V_r\rho_r C_r\frac{dT_r}{dt} &= F_r\rho_r C_r(T_{r0} - T_r) + UA(T_l - Tr),
\end{aligned}
$$

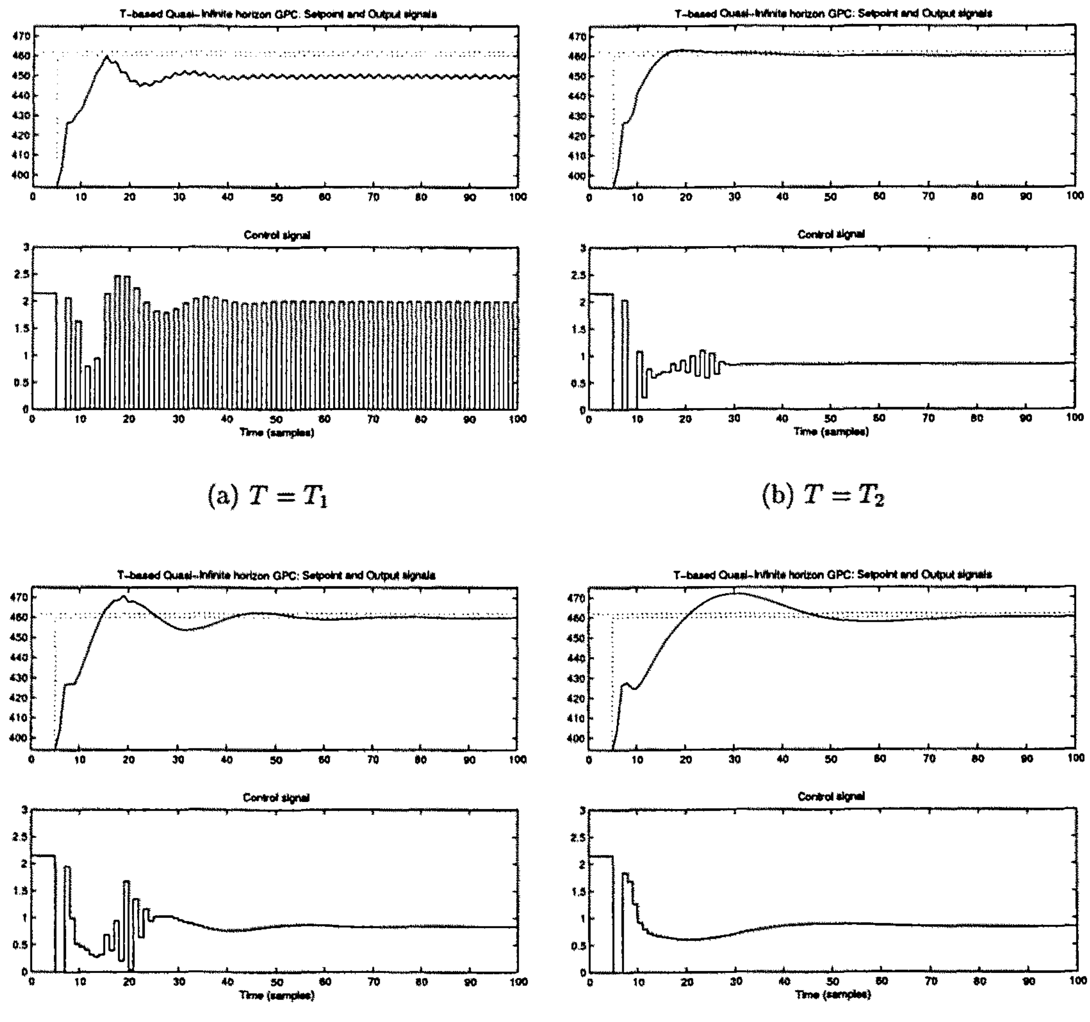


(a) $T = T_1$

(b) $T = T_2$

(c) $T = T_3$

(d) $T = T_4$

Figure C.1: Input/Output responses for the $T$-based QGPC$_1^\infty$ (solid), and output constraint (dotted)

where $F = 1$ m$^3$/min, $V = 1$ m$^3$, $k_0 = 10^{10}$ min$^{-1}$, $E_A/R = 8330.1$ K, $\rho = 10^6$ g/m$^3$, $C = 1$ cal/gK, $T_{l0} = 323$ K, $UA = 5.34 \cdot 10^6$ cal/K, $\Delta H = 1.3 \cdot 10^8$ cal/kmole, $V_r = 1$ m$^3$, $\rho_r = 10^6$ g/m$^3$, $C_r = 1$ cal/gK and $T_{r0} = 293$ K. A linearised model about the operating point $\overline{T_l} = 394$ K, $\overline{C_A} = 0.264$ kmole/m$^3$, $\overline{T_r} = 365.0333$ K and $F_r = 2.1474$ m$^3$/min has been obtained which, discretised with a sampling time of $T_s = 0.15$ min and including a ZOH at the input, becomes

$$G(q^{-1}) = \frac{q^{-1}B(q^{-1})}{A(q^{-1})} = \frac{-3.9222q^{-1} - 2.3365q^{-2} + 1.1538q^{-3}}{1 - 1.9467q^{-1} + 1.2875q^{-2} - 0.2481q^{-3}}.$$

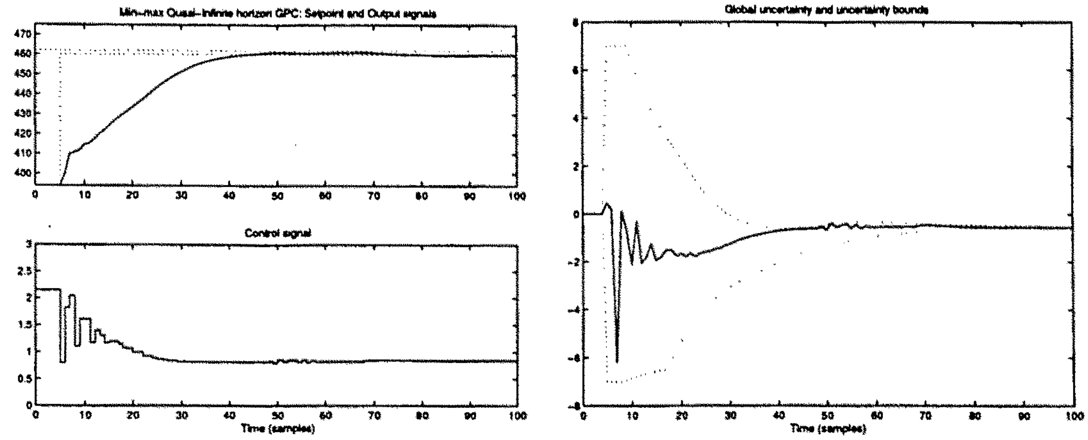


(a) Input/Output responses for the min-max QGPC$_1^\infty$ (solid) and output constraint (dotted)

(b) Global uncertainty (solid) and uncertainty bounds (dotted)

Figure C.2: Closed-loop behaviour of the min-max QGPC$_1^\infty$

In the following experiments, the setpoint is changed from $T_l = 394$ to 460 K, and the constraints $F_r \geq 0$ and $T_l \leq 462$ K are specified. For nominal performance, the tuning knobs $[N_u, \rho] = [5, 10]$ are chosen. The $T$-based QGPC$_1^\infty$ has been tuned with four classical choices of $T$, again $T_1 = 1$, $T_2 = 1 - 0.9q^{-1}$, $T_3 = A$ and $T_4 = A(1 - 0.9q^{-1})$, have been used, whereas the min-max controller has been implemented with the tuning settings $M_\theta = 10$, $\mu = 0.9$, $\theta^-(5) = -7$ and $\theta^+(5) = 7$.

Fig.C.1 shows that all the $T$-based controllers, except that which uses $T = T_1$, break the output constraint. Note that for $T = T_1$, the controller is even unable to lead the output to the setpoint and the input signal shows a permanent high-frequency oscillation. All the other choices of $T$ produce input saturation at $F_r = 0$, and the output constraint is never respected, although it is only violated by somewhat more than 1 K with $T = T_2$.

On the other hand, the min-max QGPC$_1^\infty$ is able to satisfy the input/output constraint specifications, as shown in Fig.C.2(a), and the output finally reaches the setpoint when the uncertainty bands converge to the measurements of the signal $\theta(t)$ in

Fig.C.2(b). The *whole* simulation (100 sampling instants) takes 46.7080 seconds, *i.e.* 0.4671 seconds per sampling instant, including the simulation of the system, for a 133 MHz computer.